Synthesis and characterization of ultra-thin MgO films on Mo(100)

Ming-Cheng Wu, Jason S. Corneille, Cesar A. Estrada, Jian-Wei He and D. Wayne Goodman
Department of Chemistry, Texas A&M University, College Station, TX 77843-3255, USA

Received 10 May 1991; in final form 22 May 1991

Ultra-thin MgO films have been synthesized under UHV conditions by evaporating Mg onto Mo(100) in various background pressures of oxygen. Low-energy electron diffraction (LEED) studies show that MgO films grow epitaxially in the 200–600 K substrate temperature range with the (100) face of MgO oriented parallel to Mo(100). The one-to-one stoichiometry of the MgO films has been confirmed using Auger electron spectroscopy (AES) and temperature programmed desorption (TPD). A typical loss pattern, characteristic of single-crystal MgO, has been obtained by high-resolution electron energy-loss spectroscopy (HREELS). At low oxygen pressures, the MgO film grows via a mechanism of island nucleation with domains that coexist with metallic Mg particles. The heat of sublimation of three-dimensional MgO islands is dependent on the oxygen pressure during growth and relates to the coordination number of the Mg cations.

Surface studies of metal oxides have recently attracted great interest due to their importance in heterogeneous catalysis, ceramics, photochemical reactions and in microelectronic applications. In catalysis for example, supports are often metal oxides, whereas metal oxides can also be active catalysts themselves. MgO, for example, is known to be a typical basic oxide which catalyzes the H_2 and D_2 exchange reaction [1] and the dehydrogenation of formic acid or methanol [2]. However, few surface spectroscopic studies have been carried out on well-characterized single-crystal metal-oxide surfaces [3,4]. One of the practical problems is surface charging. Most metal oxides are insulators or wide-gap semiconductors, causing charge build-up during surface spectroscopic measurements in which the probe particles are charged. This difficulty, however, can be eliminated by making an ultra-thin, well-defined, oxide film on the top of a metal substrate such that any charging induced during a charged particle measurement will dissipate into the conductive substrate.

Magnesium oxides has a rocksalt lattice, the simplest metal-oxide crystal structure, and is thus relatively easy to characterize. Accordingly, magnesium oxide has been studied both experimentally [5–7] and theoretically [8,9]. The MgO lattice contains two intersecting face-centered cubes, with each Mg^{2+} cation surrounded by six O^{2-} in a regular octahedral arrangement and each O^{2-} anion bonded by six cations. Low-energy electron diffraction (LEED) dynamical studies [6,7] have concluded that the (100) surface of MgO is very nearly a truncation of the bulk crystal structure, with any relaxation or rumpling of the surface being limited to a few percent of the bulk lattice or less.

In this Letter, we present a surface study of the growth of ultra-thin MgO films on Mo(100). Our LEED studies indicate that the MgO films grow epitaxially on Mo(100) with the (100) face of MgO oriented parallel to the (100) face of Mo. The growth mechanism and quality of the MgO films have been examined by means of Auger electron spectroscopy (AES), LEED, temperature programmed desorption (TPD) and high-resolution electron energy-loss spectroscopy (HREELS).

The studies were carried out in two UHV systems. One apparatus has capabilities for AES, LEED and TPD. HREELS was performed in a second UHV system also equipped with AES and LEED. The Mo(100) substrates could be resistively heated to 1600 K and cooled to 100 K. An electron-beam heater

0009-2614/91/$ 03.50

was mounted directly behind the specimen for heating to temperatures above 1600 K. Sample temperatures were monitored with a W–5%Re/W–26%Re thermocouple spot-welded to the edge of the rear surface. AES indicated that the main impurities on the Mo(100) surfaces were carbon and oxygen. These impurities could be removed using the following cleaning procedure: heating at 1300 K in 5×10^{-8} Torr oxygen, followed by a flash to 2000 K. After several cycles of the above procedure, a clean surface, with a sharp (1×1) LEED pattern, was obtained.

Ultra-thin MgO films were synthesized under UHV conditions by evaporating Mg onto a clean Mo(100) surface in a background pressure of oxygen. Deposition of Mg was performed by thermal evaporation of a high-purity Mg ribbon tightly wrapped around a tungsten filament. The flux of Mg evaporation was directly monitored by a mass spectrometer which was mounted in line with the Mg doser. A constant evaporation rate was achieved by adjusting the current through the tungsten filament while maintaining the Mg mass signal constant.

Mg coverages were determined by combining AES and TPD measurements. The first break point in a plot of Auger intensity versus deposition time typically correlates with the completion of the first Mg monolayer (ML). This break point in the AES plot corresponds very closely to the initial appearance of the multi-layer desorption peak of Mg from Mo(100). Moreover, our LEED studies indicate that a sharp (1×1) substrate pattern remains with increasing Mg coverage up to one ML, implying pseudomorphic growth of Mg on Mo(100). A detailed TPD, AES, XPS and LEED study of metallic Mg films grown on Mo(100) will be presented elsewhere [10].

Assuming the sticking probability of Mg atoms to the Mo(100) substrate is unity during the growth of the MgO films, the thickness of the films can be determined from the evaporation time using the calibrated Mg evaporation rate. Hereafter, a monolayer coverage of MgO corresponds to one Mg atom per substrate Mo atom. For stoichiometric MgO films, this definition also leads to one O atom per substrate atom at a monolayer coverage.

The growth of ultra-thin MgO films on the (1×1) surface of Mo was followed by AES measurements as a function of the background pressure of oxygen, as shown in fig. 1. The Mg evaporation time for each curve in fig. 1 is 20 min, corresponding to a Mg coverage of 6.8 ML. At low oxygen pressures, the metallic $Mg^0(L_{23}VV)$ transition at 44.0 eV (fig. 1a) dominates in the 20.0–60.0 eV kinetic energy region. The 44.0 eV peak decreases and a new peak at 32.0 eV becomes more predominant as the oxygen pressure is increased. The new peak is assigned to a $Mg^{2+}(L_{23}VV)$ Auger transition [11,12] due to the formation of MgO. At 1.0×10^{-7} Torr oxygen, the Mg^0 Auger transition completely disappears and only the Mg^{2+} peak remains, implying that a one-to-one stoichiometry of the MgO films has been reached. This conclusion is further supported by our LEED observations and TPD results which follow.

It is noteworthy that only two distinct peaks, $Mg^0(L_{23}VV)$ and $Mg^{2+}(L_{23}VV)$, are observed in the 25.0–50.0 eV kinetic energy region. Both the peak positions and the shapes remain unchanged as the background pressure of oxygen is varied. This behavior suggests that no intermediate sub-oxide precursors, e.g. Mg^+, are formed during Mg oxidation. The same conclusion has been reached in previous

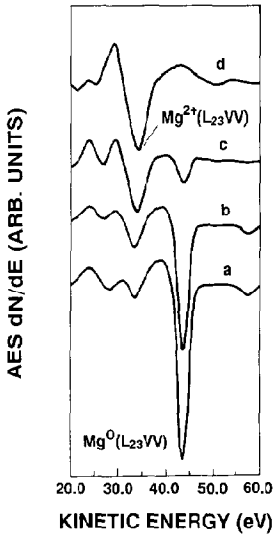

Fig. 1. Auger spectra of MgO films grown on Mo(100) at 340 K as a function of oxygen pressure: (a) 2×10^{-8} Torr; (b) 4×10^{-8} Torr; (c) 7×10^{-8} Torr; (d) 10×10^{-8} Torr. The Mg evaporation rate was maintained at 5.8×10^{12} atom cm^{-2} s^{-1} during deposition. The Mg evaporation time was 20 min for each curve, giving rise to a Mg coverage of 6.8 ML.

XPS [13] and HREELS [14] studies, where MgO films have been synthesized by oxidizing single-crystal Mg specimens.

The growth of MgO films on Mo(100) has been further examined by LEED in the 200–600 K substrate temperature range and in a background of 1.0×10^{-7} Torr oxygen. It was found that the MgO films grow epitaxially, with the (100) face of MgO oriented parallel to the Mo(100) substrate. At MgO coverages, θ_{MgO}, below one ML, the (1×1) substrate pattern remained essentially unchanged except for a slight increase in the LEED background intensity. The clouds around the sharp (1×1) integral spots appear at $\theta_{MgO}\approx2$ ML. The substrate spots were gradually attenuated and the diffraction spots from the MgO films became more intense with increasing MgO coverage. Although the substrate LEED pattern was completely attenuated at $\theta_{MgO}\approx7$ ML, a small substrate Auger feature was still detectable in the AES spectrum. Further MgO deposition eliminated this substrate signal. Fig. 2 gives two typical LEED patterns obtained from a 2.0 ML MgO film and from a 6.8 ML MgO film, respectively. For comparison, a LEED picture from a clean Mo(100) surface is also included.

In our experiments, it was found that neither subsequent annealing in oxygen pressure nor growth of the films in oxygen pressures higher than 1.0×10^{-7} Torr yielded visible improvements of the overlayer LEED patterns. This differs from a recent study of the epitaxial growth of ZrO_2 on Pt(111) [15], where post-annealing in oxygen was generally required in order to obtain a film with long-range order. Moreover, the oxygen-to-magnesium AES ratio also remained constant upon further oxidation, implying that the optimum oxidation conditions have been achieved at 1.0×10^{-7} Torr oxygen. Our LEED studies also indicate that films with long-range order can be formed in the 200–600 K substrate temperature range. The LEED observations of highly ordered MgO(100) films combined with our AES results strongly support our conclusion that near one-to-one stoichiometry of the films has been reached.

The one-to-one stoichiometry of MgO films is further confirmed by the appearance of sharp optical-phonon losses, a characteristic loss pattern for single-crystal MgO [16], obtained in HREELS as shown in fig. 3. The fundamental mode at 656 cm^{-1} and its

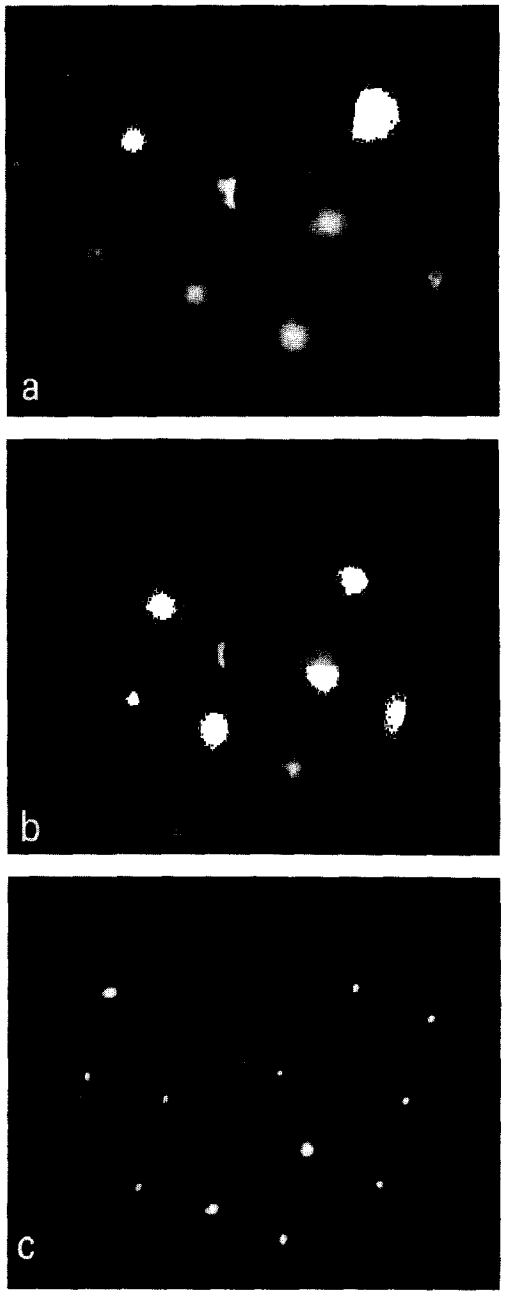

Fig. 2. LEED patterns taken from (a) a 2.0 ML MgO film, $E_p=85$ eV; (b) a 6.8 ML MgO film, $E_p=93$ eV; and (c) a clean Mo(100) surface, $E_p=146$ eV. The MgO films were grown at 340 K and the LEED photographs taken at 100 K.

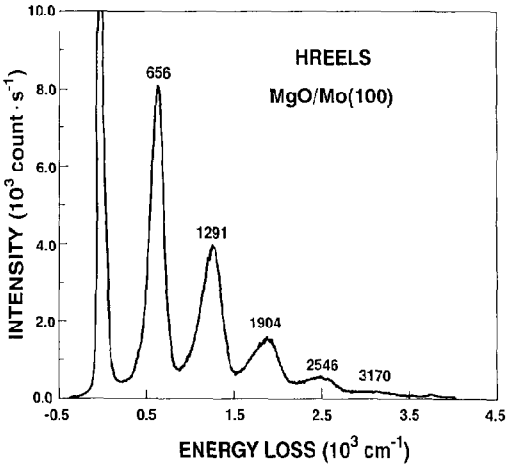

Fig. 3. HREELS spectrum obtained from a ≈ 10 ML MgO film. The spectrum is measured at a beam energy of 2 eV, with an energy resolution of 79 cm^{-1}.

multiple losses, up to the fifth loss, are evident in the spectrum.

Fig. 4 gives a typical set of TPD spectra of Mg and O mass signals acquired subsequent to the MgO film synthesis in various background pressures of oxygen. At low oxygen pressures, a sharp peak characteristic of zero-order desorption dominates the spectra (see fig. 4a). TPD studies, presented elsewhere [10], show that this peak corresponds to desorption from a Mg multi-layer. The heat of sublimation, ΔH_{Mg}, of bulk Mg derived from analysis of the thermal desorption spectrum, yields $\Delta H_{Mg} = 31.4 \pm 2.5$ kcal/mol, in good agreement with the value of 33.7 kcal/mol reported in the literature [17]. A broad peak between 600 and 1000 K in spectrum (a) of fig. 4a originates from the desorption of monolayer Mg [10]. The features at temperatures above 1000 K can therefore be attributed to desorption of MgO. As the background pressure of oxygen is increased, the metallic Mg desorption gradually diminishes and com-

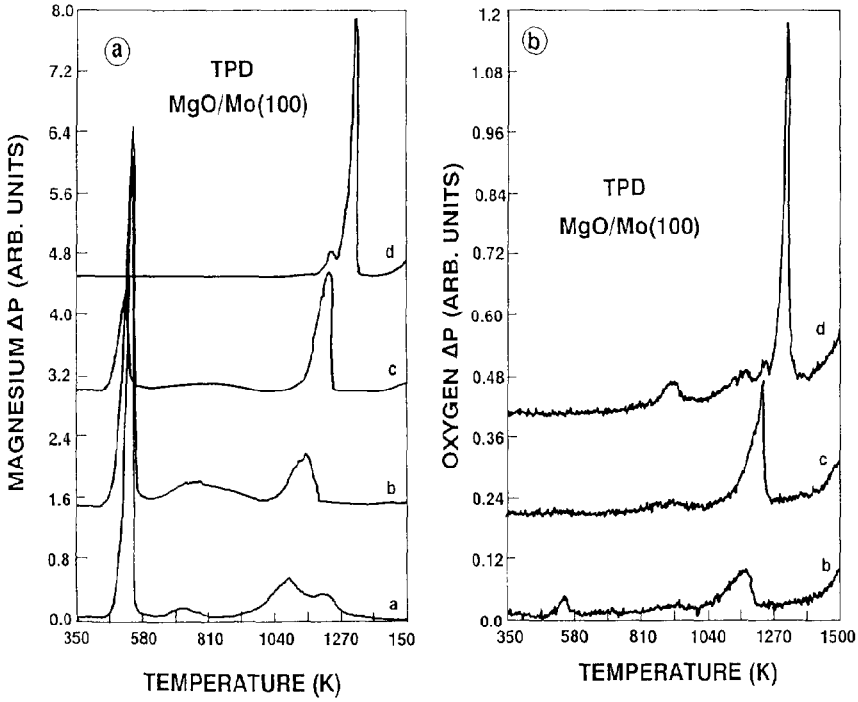

Fig. 4. (a), (b) TPD spectra of Mg and O mass signals from a MgO film synthesized as a function of background pressure of oxygen. Oxygen pressures are: (a) 2×10^{-8} Torr; (b) 4×10^{-8} Torr; (c) 7×10^{-8} Torr; (d) 10×10^{-8} Torr, respectively. The substrate temperature was 340 K during the growth of the MgO films. The Mg evaporation rate was kept at 5.8×10^{12} atom cm^{-2} s^{-1}. The Mg evaporation time was 20 min for each curve, yielding a Mg coverage of 6.8 ML.

pletely disappears at a synthesis pressure of 1.0×10^{-7} Torr oxygen, consistent with the above AES results. On the other hand, the TPD peak of MgO in fig. 4a grows and its peak position shifts to higher temperatures with increasing oxygen pressure. A similar behavior is observed for the simultaneous desorption of the oxygen counterpart of MgO, as shown in fig. 4b.

It is noteworthy that the oxide desorption peak, which is well separated from the metallic desorption peaks, has a typical shape characteristic of zero-order desorption. Therefore, the heat of sublimation, ΔH_{MgO}, of MgO films can be obtained from Arrhenius plots of the leading edge desorption rates [18]. Fig. 5 shows Arrhenius plots obtained from the corresponding MgO TPD spectra. For $\theta_{MgO}=6.8$ ML, the analysis yields $\Delta H_{MgO}=146\pm4$ kcal/mol, 10 kcal/mol higher than that previously reported [19].

Two main points can be drawn from the above TPD spectra. First, the two distinct peaks assigned to the metallic and oxide multi-layer desorption coexist in the intermediate oxygen pressure range (see fig. 4a). This feature indicates that at low oxygen pressures MgO is not formed uniformly, but rather grows via a mechanism of island nucleation. This mechanism is consistent with our AES results, where only two Mg states, Mg^0 and Mg^{2+}, are observed during oxidation. It follows also from the data of fig. 4a that oxide nucleation likely occurs directly on the Mo(100) substrate, rather than on top of a metallic Mg film. Metallic Mg covered by the oxide should yield Mg desorption features in the immediate temperature range above the oxide peak in fig. 4a. Clearly such features are not present.

Secondly, the oxide desorption peak shifts continuously towards higher temperatures with increasing background pressures of oxygen. This peak as well has the shape characteristic of zero-order desorption (see spectrum (c) of figs. 4a and 4b). The thermal desorption analysis in fig. 5 yields $\Delta H_{MgO}=109\pm2$ kcal/mol (fig. 5b). ΔH_{MgO} decreases from 146 kcal/mol in fig. 5a to 74 kcal/mol in fig. 5c. This behavior indicates that the binding strength of the octahedral cell of MgO particles formed at low oxygen pressures (less than 1.0×10^{-7} Torr oxygen) is considerably weakened. We suggest that the weakening of the binding strength is related to a decrease in the coordination number of the Mg cations in the MgO cell.

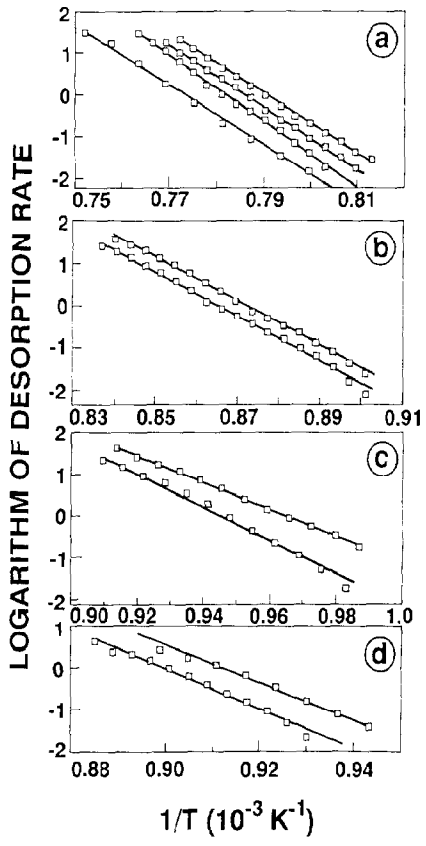

Fig. 5. Arrhenius plots obtained from the TPD of various MgO films synthesized at different oxygen pressures, P, and for varying MgO coverages. Plots in (a)–(d) were obtained from MgO films synthesized, unless noted, under the same oxidation conditions. The average values of ΔH_{MgO}, obtained from the slope of these plots, are indicated. (a) $P=1.0\times10^{-7}$ Torr, 6.8 ML MgO, $\Delta H_{MgO}=146\pm4$ kcal/mol, the lower plot was obtained from a 14.0 ML MgO film; (b) $P=7\times10^{-8}$ Torr, 6.8 ML MgO, $\Delta H_{MgO}=109\pm2$ kcal/mol; (c) $P=4\times10^{-8}$ Torr, 6.8 ML MgO, $\Delta H_{MgO}=74\pm8$ kcal/mol; (d) $P=1.0\times10^{-7}$ Torr, 2.0 ML MgO, $\Delta H_{MgO}=99\pm2$ kcal/mol.

The cation in MgO particles formed at low background pressures of oxygen may have fewer than six oxygen neighbors in the ideal crystal cell. As a consequence, the corresponding ΔH_{MgO} decreases. No attempt, however, has been made to obtain a quantitative correlation between ΔH_{MgO} and the coordination number of the Mg cations.

The above explanation is supported by the fact that ΔH_{MgO} decreases as the MgO coverage is decreased.

For example, with $\theta_{MgO}=2.0$ ML, $\Delta H_{MgO}=99\pm2$ kcal/mol (see fig. 5d). In the ideal case, the Mg cations in monolayer MgO only have four oxygen neighbors. The number of cation neighbors may further decrease with decreasing oxygen background pressure. This is evident in the TPD spectra in which ΔH_{MgO} decreases to 74 ± 8 kcal/mol at 4×10^{-8} Torr oxygen. The small shoulder whose peak desorption temperature lies below the desorption maximum in spectrum (d) of fig. 4a and fig. 4b is thus interpreted to arise from defects in the MgO film corresponding to incompletely coordinated MgO.

Combining our AES and TPD results, one additional point can be drawn: a decrease in the coordination number of the cations in the MgO films does not apparently alter significantly the oxidation state of Mg. This effective reduction in the coordination does, however, lead to an increase in the defect density, i.e. cation and anion vacancies, in the MgO particles which are in coexistence with metallic Mg. Regarding this point, it has been reported [3] that both TiO_x and VO_x exhibit the rocksalt structure for stoichiometries which vary about 1:1 by 30%. The lattices of these non-stoichiometric structures are reported to contain a large number of cation and anion vacancies.

The oxidation mechanism of single-crystal Mg surfaces has been a subject of several surface studies [11,13,14,20]. There is general agreement concerning the later stage of oxidation where thickening of the oxide layer follows the formation of an initial thin oxide film. The early stage of oxidation, however, is more controversial. A key point to be resolved is whether a chemisorbed oxygen layer serves as a precursor to the formation of the initial surface oxide. While LEED, AES, EELS and work function measurements [11,20] have suggested the existence of a chemisorbed oxygen species on metallic Mg surfaces during the initial stages of oxidation, no supporting evidence was found in XPS [13] and HREELS [14] studies. The most appealing oxidation model then is that of direct incorporation of dissociated oxygen into Mg, with concomitant formation of the oxide. A less highly coordinated oxygen species chemisorbed on the oxide surface has also been implicated [14].

The present experimental results support the latter model. However, a small desorption feature at 540 K in the oxygen TPD in spectrum (b) of fig. 4b may, in fact, arise from oxygen chemisorbed on the metallic Mg surface. The feature at 925 K, which appears in all the oxygen TPD spectra and grows as the film becomes fully oxidized, can likewise be interpreted to arise from desorption of an oxygen species chemisorbed on the oxide surface. This species is obviously less tightly bonded compared to the lattice oxygen in an octahedral cell of MgO.

In conclusion, the epitaxial growth of ultra-thin MgO films on Mo(100) has been observed by LEED. In spite of a 5.4% lattice mismatch between MgO(100) and Mo(100), a highly ordered MgO film can be formed on the substrate with its (100) face parallel to the (100) face of Mo. The AES, LEED, HREELS and TPD results all indicate that the MgO films, synthesized under the optimum oxidation conditions, have essentially a one-to-one stoichiometry. However, at low oxygen pressure and at a constant Mg evaporation rate, the MgO films grow via a mechanism of nucleation and coexist with metallic Mg particles. The heat of sublimation of the MgO particles is dependent on the oxygen pressure during growth and relates to the Mg coordination number in the oxide.

We acknowledge with pleasure the support of this work by the Department of Energy, Office of Basic Energy Sciences, Division of Chemical Science and the Gas Research Institute.

References

[1] M. Boudart, A. Delbouile, E.G. Derouane, V. Indovina and A.B. Walters, J. Am. Chem. Soc. 94 (1973) 6622.
[2] P. Mars, J.J.F. Scholten and P. Zwietering, Advan. Catalysis 14 (1963) 35.
[3] V.E. Henrich, Rept. Progr. Phys. 48 (1985) 1481.
[4] M.-C. Wu and P.J. Møller, Surface Sci. 224 (1989) 250; P.J. Møller and M.-C. Wu, Surface Sci. 224 (1989) 265.
[5] V.E. Henrich, G. Dresselhaus and H.J. Zeiger, Phys. Rev. B 22 (1980) 4764.
[6] M. Prutton, J.A. Walker, M.R. Welton-Cook and R.C. Felton, Surface Sci. 89 (1979) 95.
[7] T. Urano, T. Kanaji and M. Kaburagi, Surface Sci. 134 (1983) 109.
[8] A.J. Martin and H. Bilz, Phys. Rev. B 19 (1979) 6593.
[9] G. Lakshmi and F.W. de Wette, Phys. Rev. B 22 (1980) 5009; 23 (1981) 2035.
[10] M.-C. Wu, J.S. Corneille and D.W. Goodman, in preparation.

[11] H. Namba, J. Darville and J.M. Gilles, Surface Sci. 108 (1981) 556.
[12] V.M. Bermudez and V.H. Ritz, Surface Sci. 82 (1979) L601.
[13] J. Ghijsen, H. Namba, P.A. Thiry, J.J. Pireaux and R. Candano, Appl. Surface Sci. 8 (1981) 387.
[14] P.A. Thiry, J. Ghijsen, R. Sporken, J.J. Pireaux, R.L. Johnson and R. Caudano, Phys. Rev. B 39 (1989) 3620.
[15] V. Maurice, M. Salmeron and G.A. Somorjai, Surface Sci. 237 (1990) 116.
[16] P.A. Thiry, M. Liehr, J.J. Pireaux and R. Caudano, Phys. Rev. B 29 (1984) 4824.
[17] R.C. Weast, ed., Handbook of chemistry and physics, 67th Ed. (CRC Press, Boca Raton, 1986) p. D-45.
[18] A.M. de John and J.W. Niemantsverdriet, Surface Sci. 233 (1990) 355.
[19] G.V. Samsonov, ed., The oxide handbook (IFI/Plenum Press, New York, 1973) p. 115.
[20] S.A. Flodström and C.W.B. Martinsson, Surface Sci. 118 (1982) 513.